American Journal of Botany

RESEARCH ARTICL

Repeated evolution of a morphological novelty: a phylogenetic analysis of the inflated fruiting calyx in the Physalideae tribe (Solanaceae)

Rocío Deanna[1,2,3,4], Maximilian D. Larter[2], Gloria E. Barboza[1,2,3], and Stacey D. Smith[2]

Manuscript received 25 September 2018; revision accepted 27 November 2018.

[1] Instituto Multidisciplinario de Biología Vegetal, IMBIV (CONICET-UNC), CC 495, Córdoba 5000, Argentina

[2] Department of Ecology and Evolutionary Biology, University of Colorado, Boulder, Colorado 80305, USA

[3] Departamento de Ciencias Farmacéuticas, Facultad de Ciencias Químicas (FCQ, UNC), Medina Allende s.n., Córdoba 5000, Argentina

[4] Author for correspondence (e-mail: rociodeanna@gmail.com)

Citation: Deanna, R., M. D. Larter, G. E. Barboza, and S. D. Smith. 2019. Repeated evolution of a morphological novelty: a phylogenetic analysis of the inflated fruiting calyx in the Physalideae tribe (Solanaceae). *American Journal of Botany* 106(2): 1–10.

doi:10.1002/ajb2.1242

PREMISE OF THE STUDY: The evolution of novel fruit morphologies has been integral to the success of angiosperms. The inflated fruiting calyx, in which the balloon-like calyx swells to completely surround the fruit, has evolved repeatedly across angiosperms and is postulated to aid in protection and dispersal. We investigated the evolution of this trait in the tomatillos and their allies (Physalideae, Solanaceae).

METHODS: The Physalideae phylogeny was estimated using four regions (ITS, *LEAFY*, *trnL-F*, *waxy*) with maximum likelihood (ML) and Bayesian inference. Under the best-fitting ML model of trait evolution, we estimated ancestral states along with the numbers of gains and losses of fruiting calyx accrescence and inflation with Bayesian stochastic mapping. Also, phylogenetic signal in calyx morphology was examined with two metrics (parsimony score and Fritz and Purvis's *D*).

KEY RESULTS: Based on our well-resolved and densely sampled phylogeny, we infer that calyx evolution has proceeded in a stepwise and directional fashion, from non-accrescent to accrescent to inflated. In total, we inferred 24 gains of accrescence, 24 subsequent transitions to a fully inflated calyx, and only two reversals. Despite this lability, fruiting calyx accrescence and inflation showed strong phylogenetic signal.

CONCLUSIONS: Our phylogeny greatly improves the resolution of Physalideae and highlights the need for taxonomic work. The comparative analyses reveal that the inflated fruiting calyx has evolved many times and that the trajectory toward this phenotype is generally stepwise and irreversible. These results provide a strong foundation for studying the genetic and developmental mechanisms responsible for the repeated origins of this charismatic fruit trait.

KEY WORDS convergence; irreversibility; physaloids; stochastic mapping; trait evolution; transition rates.

Fruit evolution has long been considered a key contributor to the success of angiosperms, with bursts of morphological innovation closely tied to climatological events as well as the rise of frugivorous lineages of vertebrates (Tiffney, 1984; Eriksson et al., 2000; Knapp, 2002). Variation in fruit traits across taxa is often correlated with differences in dispersal mode (e.g., Gautier-Hion et al., 1985; Lomáscolo et al., 2010), which, in turn, can lead to shifts in diversification rates (e.g., Beaulieu and Donoghue, 2013; Lagomarsino et al., 2016; Larson-Johnson, 2016). Beyond their role in facilitating seed dispersal, fruits also serve to protect seeds from pathogens and predators (Tewksbury and Nabhan, 2001; Beckman and Muller-Landau, 2011) and promote successful germination (Traveset, 1998; Vander Wall, 2001).

From an evolutionary perspective, fruit morphology is known not only for its tremendous diversity but also for the high degree of convergence. For instance, fleshy fruits have evolved repeatedly in a wide variety of angiosperm clades—for example, Malpighiaceae (Davis et al., 2001), Rubiaceae (Bremer et al., 1995), and Solanaceae (Knapp, 2002)—often in relation to shifts in ecological niche (Bolmgren and Eriksson, 2005; Givnish et al., 2005). Even seemingly complex fruit traits, such as segmentation and seed ejection, have been gained and lost multiple times

at recent phylogenetic scales (Hall et al., 2011; Marcussen and Meseguer, 2017). Despite this evolutionary lability, relatively little is known about the extent to which convergent transitions in fruit traits occur through similar genetic and developmental mechanisms (Pabón-Mora et al., 2014; Ortiz-Ramírez et al., 2018; but see Avino et al., 2012).

Here, we focus on a charismatic but understudied fruit trait, the inflated fruiting calyx, which has evolved repeatedly across angiosperms. Inflated calyces develop by accrescence after anthesis such that the fruit becomes completely enclosed upon maturation (He et al., 2004). This feature is found in at least 11 plant families, such as Malvaceae and Lamiaceae (Paton, 1990; Padmaja et al., 2014), although it is best known from the tomato family, Solanaceae, where it is referred to as a "chinese-lantern" fruit or, more formally, the "inflated calyx syndrome" (ICS; He et al., 2004; He and Saedler, 2005; Wang et al., 2015). This enlarged fruiting calyx has been proposed to aid in dispersal by acting as a tumbleweed (Knapp, 2002) or by providing flotation in flooded environments (Wilf et al., 2017). Predispersal, the inflated calyx may also serve to protect the developing fruit from predators as well as from desiccation (Cedeño and Montenegro, 2004; Riss, 2009).

The evolution and development of inflated calyces has been studied in detail in only one clade, the tomatillos and their allies (tribe Physalideae, Solanaceae). Using comparative gene expression studies and transformation experiments, He and Saedler (2005) demonstrated that expression of a MADS-box transcription factor (*MPF2*) is required for the development of the dramatically inflated calyx in *Physalis*, and that overexpression of this gene in tomato can induce some degree of fruiting calyx accrescence. Subsequent studies across Physalideae revealed that many taxa that lack inflated calyces express *MPF2*, indicating that additional factors are required for development of the trait (Hu and Saedler, 2007). These and subsequent authors suggested that, given the shared expression of *MPF2* across Physalideae, ICS could be the ancestral state with multiple subsequent losses (Hu and Saedler, 2007; Zhang et al., 2012). Nonetheless, progress in reconstructing the history of gains and losses of this morphological innovation has been hampered by the sparse taxon sampling of Physalideae in existing phylogenies, which include only 37% of the extant taxa (Särkinen et al., 2013).

In the present study, we aim to elucidate the evolutionary history of Physalideae, which contains the vast majority of Solanaceae species with inflated calyces (146 of ~222 in total). Previous phylogenetic studies at the family level (Olmstead et al., 2008; Särkinen et al., 2013) have provided strong support for the monophyly of Physalideae and its close relationship to Capsiceae (*Capsicum* + *Lycianthes*) and Salpichroina (*Salpichroa* + *Nectouxia*). Olmstead et al. (2008) and Särkinen et al. (2013) recognized three subtribes of Physalideae: Iochrominae, Physalidinae and Withaninae, the last of which was recently proposed to include additional genera (*Deprea*, *Cuatresia*; Deanna et al., 2017). Nonetheless, many areas of the Physalideae remain unresolved—in particular, relationships within and among the genera of Physalidinae (Whitson and Manos, 2005; Zamora-Tavares et al., 2016). We seek to improve the resolution within Physalidinae and across Physalideae broadly by expanding taxon sampling (to 73% of extant species) and including additional fast-evolving markers.

In the context of this new phylogeny, we trace the evolution of fruiting calyx inflation, leveraging the wide variation in form across the clade. Within Physalideae, calyces range from non-accrescent (not increasing in size during fruit development) to highly inflated (growing to completely envelop the fruit) (Fig. 1). This variation in fruiting calyx morphology has often been used for generic delimitation (Hunziker, 2001; Sawyer, 2001; Li et al., 2013; Zamberlan et al., 2015), although phylogenetic studies suggest that these characters are homoplastic (Whitson and Manos, 2005; Hu and Saedler, 2007), resulting in several non-monophyletic genera (e.g., *Physalis* and *Chamaesaracha*; Zamora-Tavares et al., 2016). Here, we score fruiting calyx morphology across Physalideae and use statistical comparative methods to address the following questions: (1) Is fruiting calyx inflation a convergent trait in Physalideae? (2) If so, how many times has this trait been gained or lost? (3) Can lineages move directly between non-accrescent and inflated states or do they tend to transition through intermediate stages of accrescence? The answers to these questions will provide insight into the evolution of the lantern-like fruit form and lay the foundation for future studies at the genetic and developmental levels.

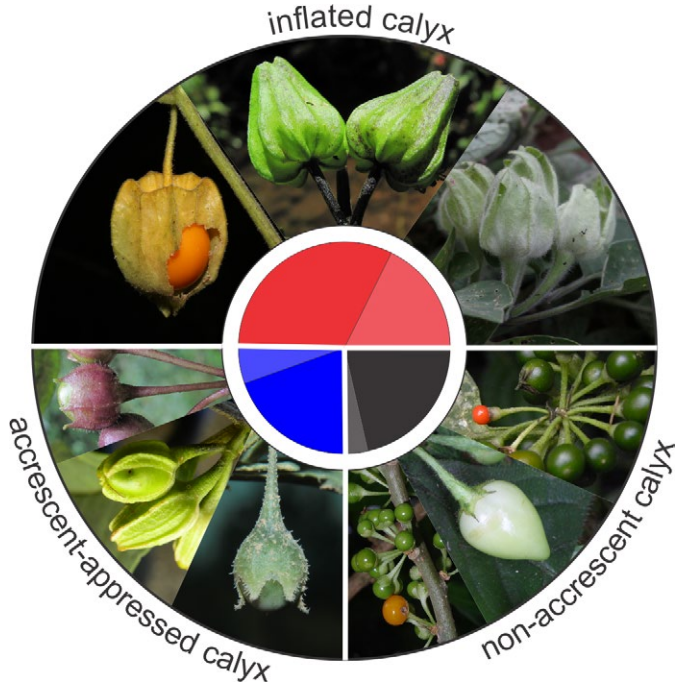

FIGURE 1. Distribution of fruiting calyx states across the tribe Physalideae. Size of pie slices represents the proportion of taxa in each state: species with inflated calyces (red, 49.7%), non-accrescent calyces (black, 24.8%), and accrescent but still appressed calyces (blue, 25.5%). The darker shade in each pie slice corresponds to the percentage of taxa with that state sampled in the present study (64.4%, 86.3%, and 77.3%, respectively). Images from red to blue (moving clockwise) are *Physalis hederifolia* (Deanna et al., 209, photo by S. Carrasco), *Deprea pumila* (Orozco et al., 3890, photo by S. Leiva González), *Aureliana cuspidata* (Stehmann et al., 6457, photo by R. Deanna), *Witheringia solanacea* (Deanna 160, photo by R. Deanna), *Aureliana wettsteiniana* (Stehmann et al., 6448, photo by R. Deanna), *Iochroma arborescens* (Orejuela & Castillo 2697, photo by A. Orejuela), *Chamaesaracha coronopus* (Deanna et al., 237, photo by S. Carrasco), *Cuatresia exiguiflora* (Orozco et al. 3853, photo by G. E. Barboza), *Deprea sawyeriana* (Deanna & Leiva González 14, photo by S. Leiva González). Photos are not to scale.

MATERIALS AND METHODS

Taxon sampling

The ingroup sampling spanned 27 of the 29 genera of Physalideae and included 215 species of the 294 species plus four varieties (Appendixes S1 and S2). The monotypic *Mellissia* and *Capsicophysalis* were the only genera not sampled. *Capsicum lycianthoides*, *Lycianthes inaequilatera*, and *Salpichroa tristis* (Appendix S1) were used as outgroups. Newly sampled plant material was either gathered from herbaria (CORD, CSU, MO, SI) or collected during several field trips to Argentina, Bolivia, Brazil, Colombia, Ecuador, Peru, and the United States in the past 10 years. Leaves were dried in silica, and vouchers were prepared and housed at local herbaria of each country (Argentina: CORD; Bolivia: LPB; Brazil: BHCB; Colombia: COL, JBB, PSO; Ecuador: LOJA, QCA, QCNE, QUSF; Peru: HAO, HUT; United States: COLO, CSU, MO). We also obtained previously extracted DNA from L. Bohs, R. Olmstead, and L. Freitas.

Phylogenetic reconstruction of Physalideae

We used de novo (407, ~55%) and published (339, ~45%) sequences from four regions to estimate relationships within Physalideae (Appendix S1, including GenBank accession numbers): the nuclear internal transcribed spacer region (ITS), the granule-bound starch synthase (GBSSI or *waxy*) gene, the second intron of *LEAFY (LFY)*, and the chloroplast spacer *trnL-F*. GBSSI regions previously sequenced by Whitson and Manos (2005) were not included in the analyses because these included exons 8–10 whereas we used exons 2–9 for most taxa. Taxon coverage was 92.8% for ITS, 77.9% for *LFY*, 78.4% for *waxy*, and 87% for the chloroplast fragment (Appendix S3). DNA extractions were done following a modified 2 × CTAB procedure (Doyle and Doyle, 1987); primers and polymerase chain reaction conditions followed previous works (Smith and Baum, 2006; Deanna et al., 2018a).

Sequence quality was inspected using GENEIOUS version 4.6.1 (Drummond et al., 2006a), and sequence alignments were performed in MEGA version 6 (Tamura et al., 2013) using the MUSCLE algorithm (Edgar, 2004) followed by manual adjustments. For *trnL-F*, a variable repeat region toward the 5′ end of the intergenic spacer was removed because this is where putative pseudogenic copies of *trnF* have been found in *Solanum* (Poczai and Hyvönen, 2011). Gene trees were estimated individually for each region with maximum likelihood (ML) in RAxML version 8 (Stamatakis, 2014) on the CIPRES server (Miller et al., 2010). We implemented the GTR + GAMMA model and used the rapid bootstrap (BS) algorithm with 1000 replicates to assess nodal support. Sequences leading to long branches were double-checked by searching for sequences highly similar to the introns and exons with BLAST in order to exclude contamination problems. Trees were then compared across genes to identify areas of hard incongruence (BS > 70%; Mason-Gamer and Kellogg, 1996).

Given the absence of hard incongruence, we conducted ML and Bayesian analyses on the combined dataset. Matrices were concatenated with SequenceMatrix version 1.8 (Vaidya et al., 2011) and partioned by gene before analysis. We also identified unstable tips based on the ML bootstrap analyses using the software RogueNaRok (Aberer et al., 2013). Two iterations of RogueNaRok were run with settings according to Särkinen et al. (2013), and rogue taxa were removed after each iteration, resulting in the pruning of 10 tips in total.

The final combined matrix included 7988 bp of aligned sequences of 222 taxa, including outgroups. We performed ML phylogenetic inference partitioned by gene using RAxML according to the parameters used for individual region analyses (see above) on the CIPRES server (Miller et al., 2010). Bayesian analyses were conducted for the combined dataset with four partitions in BEAST version 2 (Bouckaert et al., 2014), also on the CIPRES server. Best models of substitution were incorporated for each partition according to a previous selection with the Akaike information criterion (AIC) using jModelTest version 2.1.3 (Appendix S3; Posada and Crandall, 1998; Darriba et al., 2012). Two independent BEAST analyses were run for 50 million generations each with tree sampling every 1000 generations, using an uncorrelated lognormal relaxed clock model to describe the branch-specific substitution rates (Drummond et al., 2006b). We used a birth–death tree prior, which accounts for both speciation and extinction (Gernhard, 2008), and a constraint of monophyly for all species excluding *Salpichroa tristis* (the outgroup most distantly related to Physalideae). Convergence and stationarity of the parameters were inspected using Tracer version 1.7 (Rambaut et al., 2018), targeting minimum effective sample sizes ≥200. The initial 20% of trees were discarded as burn-in, and the results were combined using LogCombiner as implemented in the BEAST package. The phylogenetic relationships were summarized in a maximum clade credibility (MCC) tree, and the posterior probabilities (PP) for all nodes were derived using TreeAnotator version 2.4.7. The trees were visualized in FigTree version 1.4.3 (Rambaut, 2016).

Character coding of fruiting calyces

Fruiting calyces from taxa included in the phylogeny were scored using specimens housed at herbaria (COL, COLO, CORD, CSU, MO, SI), the JSTOR Plants database, and the literature (Appendix S2). Following Hu and Saedler (2007), we scored a fruiting calyx as accrescent-appressed when there is an increase in calyx length ≥50% from flower to fruit stage (e.g., *Brachistus stramoniifolius*) or the berry is entirely covered but there is not a space between calyx and berry (e.g., *Cuatresia exiguiflora*). Fruiting calyx was coded as non-accrescent when it grows <50% from flower to fruit stage (e.g., *Witheringia solanacea*), and as inflated when the fruit is entirely enclosed by the calyx and there is also a space between calyx and berry (e.g., *Physalis peruviana*; see matrix in Appendix S4). Note that following this definition, species of *Iochroma* are coded as non-accrescent despite being described as often having accrescent calyces (Hunziker, 2001; Smith and Baum, 2006; Lezama Escobedo et al., 2007; Cueva Manchego et al., 2015). In *Iochroma*, accrescence is usually <50% of the length present at the flowering stage. In a handful of species (e.g., *I. calycinum*, *I. barbozae*; Khan et al., 2012a; Leiva González et al., 2013), the fruiting calyx covers the berry (or nearly so), but this is due to the large size of the flowering calyx.

Testing for phylogenetic signal

We implemented two metrics to examine the level of phylogenetic signal in fruiting calyx morphology. First, we calculated the parsimony score using the "parsimony" function in the R package "phangorn" (Schliep, 2011). This metric represents the minimum number of changes necessary to describe the trait distribution on the tree. Second, we computed Fritz and Purvis's *D* (FPD; Fritz and Purvis, 2010), a metric that captures the sum of sister clade differences, also available in "phangorn". The FPD statistic takes a value of one if the

trait has a phylogenetically random distribution, and a value of zero if the trait has evolved under Brownian motion, whereby shared history will lead closely related taxa to have similar trait values. For both measures, we tested whether the observed values differed from those expected by chance (no phylogenetic signal) as well as those expected under Brownian motion. In the former case, the null distribution was created by randomly reshuffling the tip states 1000 times, and in the latter case, by evolving these traits on the phylogeny under a Brownian motion model 1000 times. These null distributions were created with the "treestat" function in the "phylometrics" package (Hua and Bromham, 2016). Traits with phylogenetic signal differ significantly from the random distribution ($P < 0.05$) but not the distribution expected under Brownian motion. As the FPD statistic can only be applied to binary traits, we considered fruit accrescence and inflation separately (Appendices S5 and S6), while for parsimony, we were able to examine them jointly as a three-state character (Fig. 1). These analyses were conducted using the MCC tree.

Reconstructing the evolutionary transitions to fruiting inflated calyces

We estimated the history of fruit calyx evolution across Physalideae using ML and Bayesian approaches. We first compared the fit of alternative models of trait evolution using the "ape" package in R (Paradis et al., 2004) and the MCC tree from the BEAST analyses. We considered six models, with the first having transition rates between all states free to vary (the all rates different model) and the second having all rates equal. We then fit four stepwise models, where lineages move from non-accrescent to inflated through the intermediate state of accrescent-appressed. Model 3 has all steps being reversible, while the last three models have one or more of these steps constrained to be irreversible (Table 1). Model selection was conducted with the AIC score, with the best model having a score at least two AIC units lower than the model with the next lowest AIC score (Burnham and Anderson, 2002).

Using the best-fitting model, we next estimated ancestral states and the number of transitions between states with Bayesian stochastic mapping (SM). Through rounds of simulation ("realizations"), SM generates a sample of histories of discrete character evolution on a phylogeny that should approximate the posterior distribution of histories (Huelsenbeck et al., 2003). In order to incorporate phylogenetic uncertainty, we performed 500 simulations of character history on a sample of 100 trees from the BEAST analysis with the combined dataset. The simulations, carried out with the "make.simmap" function in the "phytools" package (Revell, 2012), were summarized on the MCC tree to provide the posterior probability of each state at each node. We also estimated the median number of changes for each transition type from the histories and computed 95% credibility intervals using the "hdr" (highest density region) function from the "diversitree" package in R (FitzJohn, 2012).

TABLE 1. Comparison of likelihood models tested for fruiting calyx accrescence and inflation, including log-likelihood (lnLik) and Akaike information criterion (AIC) scores. The lowest AIC score is in bold. Character states: 0 = non-accrescent, 1 = accrescent-appressed, 2 = inflated fruiting calyx; thus, q_{01}, for example, denotes the transition rate from non-accrescent to accrescent-appressed.

Model tested	Constraints	Free parameters	lnLik	AIC
1. All rates different	–	6: q_{01}, q_{10}, q_{02}, q_{20}, q_{12}, q_{21}	−109.364	230.727
2. Equal rates	$q_{01} = q_{10} = q_{02} = q_{20} = q_{12} = q_{21}$	1: q	−123.646	249.291
3. Stepwise reversible	$q_{02} = 0$, $q_{20} = 0$	4: q_{01}, q_{10}, q_{12}, q_{21}	−109.374	226.747
4. Stepwise 0–1 irreversible	$q_{02} = 0$, $q_{20} = 0$, $q_{10} = 0$	3: q_{01}, q_{12}, q_{21}	−109.374	**224.747**
5. Stepwise 1–2 irreversible	$q_{02} = 0$, $q_{20} = 0$, $q_{21} = 0$	3: q_{01}, q_{12}, q_{10}	−111.630	229.259
6. Stepwise irreversible	$q_{02} = 0$, $q_{20} = 0$, $q_{21} = 0$, $q_{10} = 0$	2: q_{01}, q_{12}	−111.630	227.259

RESULTS

Phylogeny of Physalideae

Our final combined matrix had a taxon coverage of 84% (Appendix S3) and comprised 215 species of Physalideae. This represents 73.1% of the total species within the tribe and 55% of the species within *Physalis*. The plastid *trnL-F* and the nuclear region ITS were the most densely sampled, whereas ITS contributed most parsimony-informative characters (Appendix S3). Hard incongruence was not found among gene trees (Appendix S7). The ML and Bayesian topologies were largely congruent (Fig. 2 and Appendix S8, respectively) and showed strong to moderate support for Physalidinae (BS = 63%, PP = 1) and Iochrominae (BS = 100%, PP = 1), which is resolved as sister to the remaining Physalideae taxa (BS = 89%, PP = 1). The previously proposed subtribe Withaninae (Olmstead et al., 2008; Särkinen et al., 2013) does not appear to be monophyletic but instead was divided between two clades, with the Hawaiian *Nothocestrum* and allied Old World genera more closely related to Physalidinae than other members of Withaninae. Moreover, eight of the 27 sampled genera are non-monophyletic as presently circumscribed (e.g., *Iochroma*, *Cuatresia*, *Physalis*).

Testing for phylogenetic signal of accrescent and inflated fruiting calyces

We found strong phylogenetic signal for fruiting calyx accrescence and inflation with both implemented approaches. These traits have a significantly lower parsimony score and lower FPD compared to the random null distribution, suggesting that species with accrescent and inflated calyces are more closely related than expected by chance (Table 2). Consistent with this result, neither of the traits significantly differed from expectations under a Brownian motion model of evolution, which makes closely related taxa more likely to exhibit the same state due to their shared history (Table 2).

Evolutionary transitions to fruiting inflated calyces

The best-fitting ML model for fruiting calyx evolution was the stepwise model with transitions between accrescent and non-accrescent fruiting calyces being irreversible (reverse transition rate not different from zero). This model had the lowest AIC score and was greater than two AIC units lower than any competing model (Table 1;

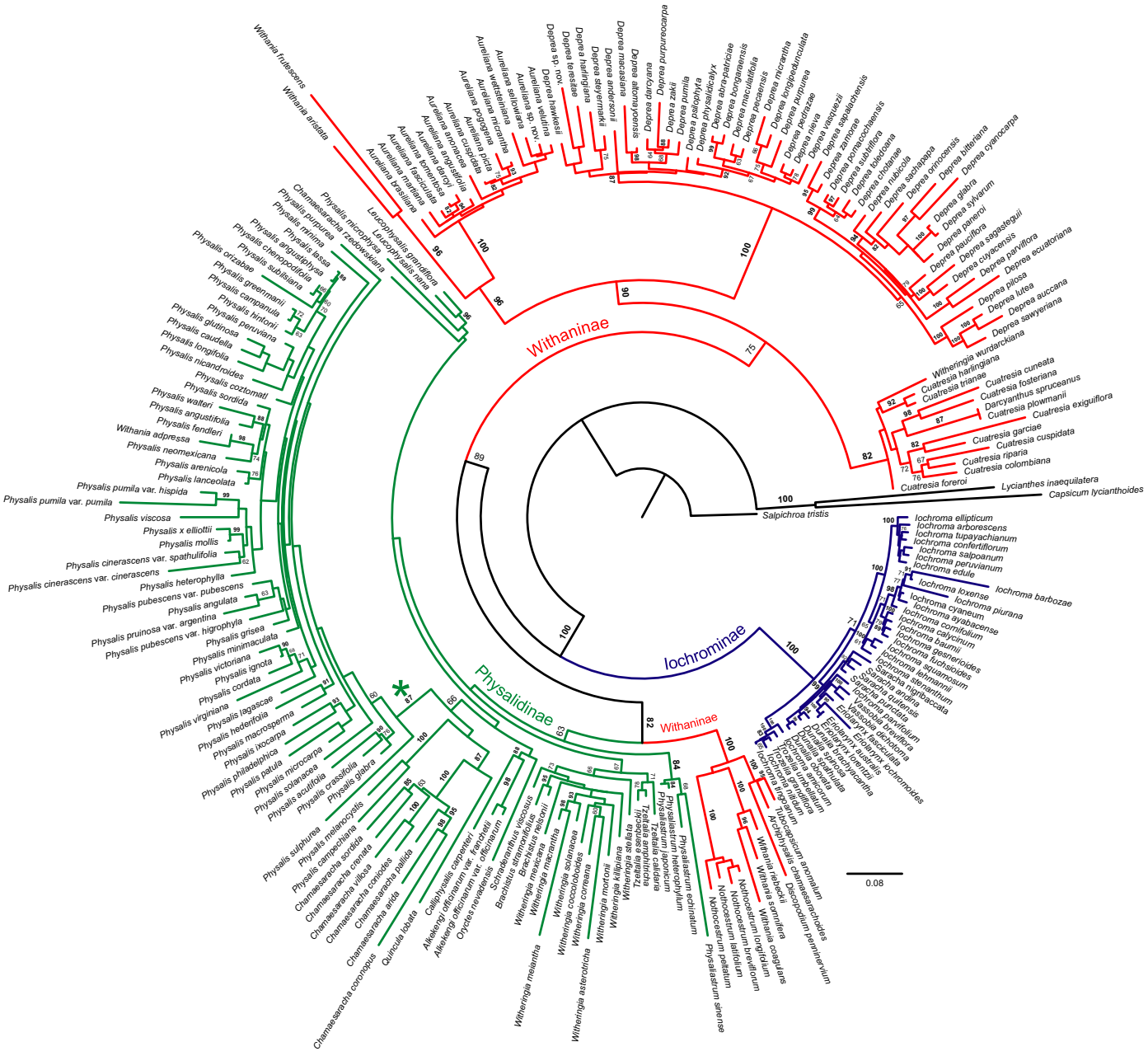

FIGURE 2. Phylogenetic relationships of Physalideae based on a maximum likelihood analysis of the combined dataset of four markers (ITS, *LFY*, *trnL-F*, and *waxy*). Bootstrap support (BS) values >60% are given above each branch, and bold numbers indicate BS > 80%. Differently colored branches correspond to the subtribes proposed by Olmstead et al. (2008), followed by Särkinen et al. (2013) and modified by Deanna et al. (2017). The asterisk indicates *Physalis* subg. *Rydbergis*.

Appendix S9). Our stochastic mapping simulations with this model estimated a median of 50 changes across the clade (95% credibility interval [CI]: 44.56–56.04). Among these changes, shifts from non-accrescent to accrescent-appressed calyces and accrescent-appressed to inflated calyces were inferred to occur at roughly equal frequencies (median = 24, 95% CI: 19.94–29.09 vs. median = 24, 95% CI: 19.96–27.71; Appendix S10). Loss of inflation to an accrescent-appressed calyx was infrequent (median = 2, 95% CI: 0–3.93; Appendix S10). The ancestral state of the tribe was estimated by SM as non-accrescent in all stochastic maps (100% posterior probability; Fig. 3). Similarly, high support was inferred for this ancestral state at many nodes throughout the phylogeny, revealing multiple independent gains of accrescence and inflation (Fig. 3).

DISCUSSION

Phylogenetic relationships and taxonomy of Physalideae

We present the first well-resolved and densely sampled phylogeny of the Physalideae tribe. This dataset is a significant expansion compared with previous studies (e.g., 33 species of *Physalis*

TABLE 2. Phylogenetic signal for fruiting calyx accrescence. All characters show significant signal (i.e., have parsimony scores and FPD values that are significantly lower than observed under the random distribution; bold values, $P < 0.05$) but are not significantly different from the distribution under Brownian motion ($P > 0.05$). Note that FPD can adopt negative values up to −0.5 when the phylogenetic signal is high (Fritz and Purvis, 2010).

Trait	Parsimony score (PS)	*P* value of observed vs. random distribution	*P* value of observed vs. Brownian motion evolution	Fritz and Purvis's *D* (FPD)	*P* value of observed vs. random distribution	*P* value of observed vs. Brownian motion evolution
Fruiting calyx accrescence and inflation	33	**0.000**	0.910	NA	NA	NA
Fruiting calyx accrescence	14	**0.000**	0.960	**−0.483**	**0.002**	0.961
Fruiting calyx inflation	20	**0.003**	0.934	**−0.356**	**0.000**	0.949

in Zamora-Tavares et al., [2016;] vs. 53 taxa here), and the sampling covers most of the taxonomic, morphological, and geographic variation within this group. Our results point to multiple taxa in need of re-circumscription, underscoring the importance of phylogenetic work to inform taxonomic revision (e.g., Olmstead et al., 2008). Although some parts of the tree (e.g., within *Physalis*) will require additional data for better resolution, our results have recovered many previously proposed relationships as well as several new ones, which we briefly review below. Taxonomic changes based on these results and an extensive revision of herbarium collections will be forthcoming in our future work.

Starting with the monophyletic and well-studied Iochrominae, only three out of six genera are monophyletic, even after recent nomenclatural changes (Shaw, 2018a, b). The crossability among genera, high convergence in traits used to delimitate generic taxonomy, and the comparative lack of karyological variation (Smith and Baum, 2006; Smith et al., 2008; Deanna et al., 2018b; Shaw, 2018b) suggest that combining the genera into a single monophyletic *Iochroma* may be the most stable solution. During the past 20 years, 19 new species of *Iochroma* and one *Saracha* have been described (e.g., Leiva Gonzalez et al., 2003; Leiva González and Lezama, 2005; Lezama Escobedo et al., 2007; Fernandez-Hilario and Smith, 2017), but no key for the entire group has been proposed, increasing the necessity of a full taxonomic revision.

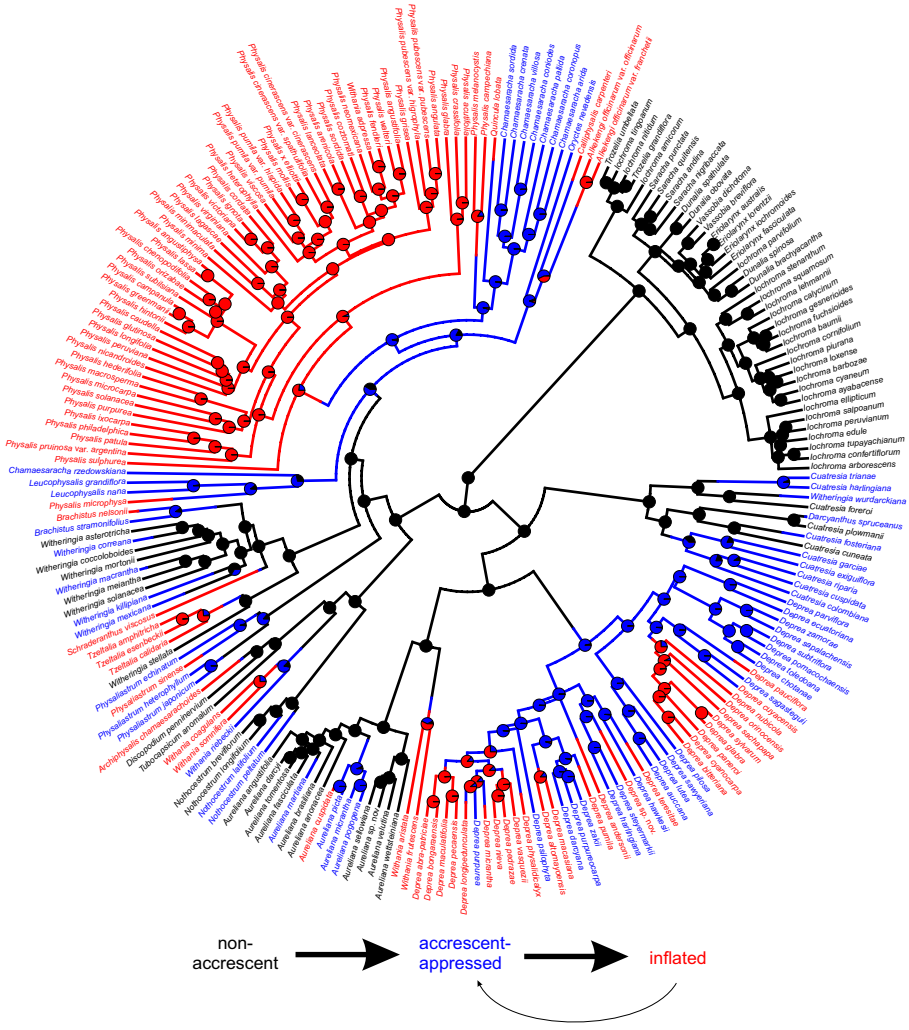

FIGURE 3. Reconstruction of fruiting calyx evolution in the Physalideae tribe. Topology is provided from four-gene BEAST analyses of 219 taxa. Circles at nodes indicate the posterior probabilities from stochastic mapping and tip label colors represent tip states, with red, blue, and black representing inflated, accrescent-appressed, and non-accrescent fruiting calyces, respectively. On the bottom, transitions between states are represented with arrows proportional to the number of estimated changes (see Appendix S10).

The subtribe Withaninae also presents taxonomic challenges, at both the subtribal and generic levels. This subtribe was originally circumscribed by Olmstead et al. (2008) to contain seven small genera, which were all Old World except for the South American *Aureliana*. Deanna et al. (2017) placed the re-circumscribed *Deprea* within Withaninae and suggested that *Cuatresia* could also be included, based on the phylogeny. Our analysis provides strong support for the close relationship of *Aureliana* to *Cuatresia* and *Deprea*, but also for the non-monophyly of the type genus, *Withania*, with three species (*W. coagulans*, *W. riebeckii*, and *W. somnifera*)

closely related to other taxa in Withaninae *sensu* Olmstead et al. (2008), and the other two species (*W. aristata* and the type species *W. frutescens*) closely related to *Aureliana*. In a prescient review, Hepper (1991) pointed out that these two western African species, *W. aristata* and *W. frutescens*, are morphologically unlike others in *Withania* and suggested that their closest relatives may instead be across the Atlantic. Beyond the rearrangement of Withaninae necessitated by this apparent split within *Withania*, most of the genera that have been placed in the subtribe are monophyletic (or nearly so), based on extensive taxonomic work in recent years (Zamberlan et al., 2015; Deanna et al., 2018a).

The largest subtribe Physalidinae, with 12 genera, was recovered as a monophyletic group, although relationships among and within the genera are complex and, in some cases, unresolved. One complicating factor is the large number of monotypic genera (*Alkekengi*, *Calliphysalis*, *Oryctes*, *Quincula*, *Schraderanthus*), some of which are nested within other genera. Nonetheless, several of the affinities that we uncovered have been proposed by previous authors using morphological data—for example, between *Brachistus* and *Witheringia* (Hunziker, 1969) and between xerophytic *Chamaesaracha* but excluding *C. rzedowskiana* (Averett, 1973; Turner, 2015)—suggesting viable avenues for future taxonomic rearrangements. Perhaps the greatest challenge will be estimating relationships within *Physalis*, which remain largely unclear in the present study, as they have in previous analyses (Whitson and Manos, 2005; Zamora-Tavares et al., 2016). The lack of resolution within this clade may reflect a history of rapid diversification and hybridization, which will likely be elucidated only with phylogenomic approaches (e.g., Stenz et al., 2015).

Repeated evolution of fruiting calyx accrescence and inflation

Our analyses demonstrate that the highly inflated fruiting calyx considered so characteristic of *Physalis* has evolved repeatedly in Physalideae. While previous studies had suggested homoplasious patterns in fruiting calyx variation in the tribe (Whitson and Manos, 2005; Hu and Saedler, 2007), we provide the first estimates of the numbers of gains and losses, with approximately 24 gains of accrescence, 24 subsequent gains of inflation, and two reversals from inflation to the accrescent-appressed state (Fig. 3). Despite these many gains of calyx accrescence and inflation, we recovered significant phylogenetic signal in these traits overall. Indeed, the character states appear clustered on the phylogeny, with some large clades (e.g., Iochrominae, *Physalis* subg. *Rydbergis*) being invariant in the degree of fruiting calyx accrescence.

The many independent origins of calyx inflation may have occurred through recurring modifications of the shared underlying pathway, which is well studied in several Physalideae. The development of ICS requires the expression of *MPF2*-like MADS-box transcription factors in flowering calyces (He and Saedler, 2005). Nonetheless, *MPF2* expression in the calyx is widespread across taxa with and without ICS in Physalideae and even in Capsiceae (Hu and Saedler, 2007), suggesting that the development of ICS is determined by other factors. Indeed, the effect of *MPF2* on calyx morphology appears to hinge on interactions with cytokinin and gibberellin, which are released upon fertilization (He and Saedler, 2007; Khan et al., 2012b). Thus, genetic changes that modify these hormonal signals, *MPF2* expression, or *MPF2* function could all contribute to variation in calyx inflation (Riss, 2009). Comparative molecular and developmental studies to date implicate both regulatory and structural mutations in *MPF2*-like genes (Hu and Saedler, 2007; Khan et al., 2009; Riss, 2009), coupled with shifts in copy number due to the many ploidy changes in the tribe (Iqbal and Datta, 2007; Deanna et al., 2018b).

Inflated calyces have convergently evolved in many taxa outside of Solanaceae, although the possibility that these rely on the same genetic pathway has not been explored. The 11 families with highly accrescent calyces, in which the fruits may be berries, drupes, or capsules, are spread across eudicots, from rosids (e.g., Caryophyllaceae, Malvaceae, Aptandraceae) to asterids (e.g., Lamiaceae, Boraginaceae, Campanulaceae) (Paton, 1990; Francis, 2000; Gottschling and Miller, 2006; Wilf et al., 2017). Solanaceae is the only family in which the developmental genetics of the trait has been studied in detail (Wang et al., 2015). Intriguingly, however, overexpression of *MPF2*-like genes in *Arabidopsis* results in enlarged and persistent calyces (Khan et al., 2013), and the *MPF2*-like promoters from Physalideae are able to drive sepal-specific gene expression, also in *Arabidopsis* (Khan et al., 2012b). These patterns suggest that many elements of networks regulating sepal growth are widely conserved, raising the possibilty that the evolution of inflated calyces in other clades has involved similar mechanisms.

Loss vs. gain of inflation through a stepwise model of evolution

Our comparative analyses indicate that evolution of the inflated calyx proceeds in directional fashion, starting from the non-accrescent state, moving first to an accrescent but appressed state before finally becoming inflated. This pattern contradicts the hypothesis that, given the complex developmental pathway required to produce ICS, inflation should be easier to lose than to gain (Hu and Saedler, 2007). These frequent and directional transitions toward inflation suggest not only that the trait is genetically accessible (perhaps given the background of *MPF2* expression in Physalideae calyces), but also that inflation is generally retained by lineages in which it evolves. Still, the adaptive advantages that could favor the fixation of this trait (e.g., protection from desiccation, deterrence of predators, enhanced dispersal) are largely untested (but see Wilf et al., 2017). In fact, the only evidence for adaptive evolution of ICS comes indirectly from molecular studies, which have estimated positive selection acting on *MPF2*-like genes in *Withania* and *Physalis* (Khan et al., 2009; Zhang et al., 2012).

The retention of ICS following its evolution may reflect not only selective advantages, but also developmental constraints acting on reversals. Ablation experiments in two ICS taxa (*Physalis* and *Withania*) reveal a complex crosstalk between calyx and fruit development at early stages, wherein removal of sepals prior to fertilization completely abolishes fruit setting (He and Saedler, 2007; Khan et al., 2012b); even ablations at later stages result in the development of smaller berries. These results suggest that genetic changes that reduce sepal size in ICS taxa might also reduce fruit size, which would presumably carry negative consequences for plant fitness. In the future, it would be valuable to conduct similar ablation experiments across Physalideae with non-accrescent, accrescent-appressed, and inflated calyces to determine whether the negative effect of calyx damage on fruit development scales with the degree of accrescence of the fruiting calyx.

Despite the strong directionality inferred from our analyses, it is important to note that such patterns may be confounded by state-dependent differential diversification. For example, the abundance of inflated calyces (as in Physalideae) can occur through biased transitions toward this state or by increased diversification

of lineages with the state (Ng and Smith, 2014). A thorough analysis of the effects of calyx evolution on speciation and extinction rates will require a larger phylogeny (Beaulieu and O'Meara, 2016), ideally at the family level and including all of the remaining genera (six) and species (76) with ICS. Diversification analyses would also benefit from new divergence time estimates in light of the recent discovery of Eocene lantern fruit fossils (Wilf et al., 2017). These fossils, placed in crown group *Physalis*, are dated to 52.2 mya, which is roughly the age inferred for the entire crown group Solanaceae in previous work (Särkinen et al., 2013; De-Silva et al., 2017). This contrast highlights the need for a complete reassessment of Solanaceae fossils (Särkinen et al., 2013, 2018; Wilf et al., 2017), together with a new family-wide dating analysis including all reliable fossil taxa.

CONCLUSIONS

Our phylogeny provides a starting point for re-circumscription of taxa and lays the foundation for ongoing research into morphological diversification of Physalideae and its spread around the globe. The charismatic lantern fruits, characteristic of the genus *Physalis*, have evolved repeatedly among its close relatives in Physalideae. In each case, lineages have moved stepwise toward the inflated calyx, with many extant lineages exhibiting intermediate states of accrescence. This well-resolved evolutionary history for Physalideae, together with the growing knowledge of fruit developmental pathways, will facilitate future work to trace the genetic changes that lead to ICS and may also explain the apparent directionality of transitions toward this morphological novelty.

ACKNOWLEDGEMENTS

The authors thanks L. Bohs, L. Freitas, and R. D. Olmstead for DNA samples; J. Stone, C. Carrizo García, Z. Zhang, E. Sessa, and F. Chiarini for leaf samples; and herbaria staff from COLO, CORD, FLAS, MO, and SI for permission to extract leaf samples from specimens. We also greatly appreciate the help of C. Pretz, S. Carrasco, A. Orejuela, and L. Fernández during fieldwork, and the insightful suggestions of J. Ng on R scripts. Photos were kindly provided by A. Orejuela, S. Carrasco, and S. Leiva González; and S. Liu was very helpful with translating Chinese for Asian taxa. The authors gratefully acknowledge support from the National Science Foundation (grant no. 1553114 to S.D.S.), Consejo Nacional de Investigaciones Científicas y Técnicas (CONICET, grant PIP 00147), Agencia Nacional de Promoción Científica y Tecnológica (FONCyT, grant PICT 2017-2370), and SECyT (Res. 411-18, Universidad Nacional de Córdoba, Argentina). R.D. also thanks Fulbright and Ministerio de Educacion y Deportes (Argentina) for grants to perform molecular studies at the University of Colorado at Boulder, and IDEAWILD for the equipment provided for fieldwork. We also appreciate the insightful comments provided by two anonymous reviewers.

AUTHOR CONTRIBUTIONS

R.D. and S.D.S. designed the study. R.D. and S.D.S. extracted DNA and performed polymerase chain reaction. R.D. analyzed sequences and performed alignments and phylogenetic analyses. R.D. and M.D.L. applied phylogenetic comparative methods. R.D. and S.D.S. wrote the paper, with contributions from M.D.L. and G.E.B.

DATA ACCESSIBILITY

All sequences have been deposited in GenBank (http://www.ncbi.nlm.nih.gov/genbank) with accessions numbers and voucher information detailed in Appendix S1. Gene trees are presented in Appendix S7.

SUPPORTING INFORMATION

Additional supporting information may be found online in the Supporting Information section at the end of the article.

APPENDIX S1. Summary of taxon sampling, provenance, voucher, and GenBank accession numbers.

APPENDIX S2. Total number of species per genus, including the distribution for each fruiting calyx character state (inflated, accrescent-appressed, and non-accrescent) and proportion of species sampled.

APPENDIX S3. Matrix information. List of the four regions used for building the Physalideae phylogeny, showing level of sampling, aligned length of matrix, variable sites per region, and proportion of parsimony informative characters.

APPENDIX S4. Matrix with the scoring of all species sampled as non-accrescent, accrescent-appressed, or inflated fruiting calyx.

APPENDIX S5. Matrix with the scoring of all species sampled as non-accrescent or accrescent fruiting calyx.

APPENDIX S6. Matrix with the scoring of all species sampled as non-inflated or inflated fruiting calyx.

APPENDIX S7. Phylogenetic relationships of Physalideae based on a maximum likelihood analysis of each marker (ITS, *LFY*, *trnL-F*, and *waxy*).

APPENDIX S8. Maximum clade credibility (MCC) tree of Physalideae obtained from a Bayesian analysis of the combined dataset of four markers (ITS, *LFY*, *trnL-F*, and *waxy*).

APPENDIX S9. Transition rates estimated for different models tested for fruiting calyx accrescence and inflation evolution in Physalideae, using a maximum likelihood analysis with the "ace" function from the "ape" package.

APPENDIX S10. Summary of the stochastic character mapping for fruiting calyx accrescence and inflation, using the best estimated model (stepwise with irreversible 0–1 transition).

LITERATURE CITED

Aberer, A. J., D. Krompass, and A. Stamatakis. 2013. Pruning rogue taxa improves phylogenetic accuracy: An efficient algorithm and webservice. *Systematic Biology* 62: 162–166.

Averett, J. E. 1973. Biosystematic study of *Chamaesaracha* (Solanaceae). *Rhodora* 75: 325–365.

Avino, M., E. M. Kramer, K. Donohue, A. J. Hammel, and J. C. Hall. 2012. Understanding the basis of a novel fruit type in Brassicaceae: Conservation and deviation in expression patterns of six genes. *EvoDevo* 3: 20.

Beaulieu, J. M., and M. J. Donoghue. 2013. Fruit evolution and diversification in campanulid angiosperms. *Evolution* 67: 3132–3144.

Beaulieu, J. M., and B. C. O'Meara. 2016. Detecting hidden diversification shifts in models of trait-dependent speciation and extinction. *Systematic Biology* 65: 583–601.

Beckman, N. G., and H. C. Muller-Landau. 2011. Linking fruit traits to variation in predispersal vertebrate seed predation, insect seed predation, and pathogen attack. *Ecology* 92: 2131–2140.

Bolmgren, K., and O. Eriksson. 2005. Fleshy fruits–origins, niche shifts, and diversification. *Oikos* 109: 255–272.

Bouckaert, R., J. Heled, D. Kühnert, T. Vaughan, C.-H. Wu, D. Xie, M. A. Suchard, et al. 2014. BEAST 2: A software platform for Bayesian evolutionary analysis. *PLoS Computational Biolology* 10: e1003537.

Bremer, B., K. Andreasen, and D. Olsson. 1995. Subfamilial and tribal relationships in the Rubiaceae based on *rbcL* sequence data. *Annals of the Missouri Botanical Garden* 82: 383–397.

Burnham, K. P., and D. R. Anderson. 2002. Model selection and multimodel interference. Springer, New York, New York, USA.

Cedeño, M. M., and D. M. Montenegro. 2004. Plan exportador, logistico y de comercializacion de uchuva al mercado de Estados Unidos para frutexpo SCI Ltda. Bachelor's thesis, Facultad de Ingeniería, Pontificia Universidad Javeriana, Bogotá, Cundinamarca, Colombia.

Cueva Manchego, M. A., S. D. Smith, and S. Leiva González. 2015. A new and endangered species of *Iochroma* (Solanaceae) from the cloud forests of central Peru and its Phylogenetic position in Iochrominae. *Phytotaxa* 227: 147–157.

Darriba, D., G. L. Taboada, R. Doallo, and D. Posada. 2012. jModelTest 2: More models, new heuristics and parallel computing. *Nature Methods* 9: 772.

Davis, C. C., W. R. Anderson, and M. J. Donoghue. 2001. Phylogeny of Malpighiaceae: Evidence from chloroplast ndhF and trnL-F nucleotide sequences. *American Journal of Botany* 88: 1830–1846.

Deanna, R., G. E. Barboza, and C. Carrizo García. 2017. Phylogenetic relationships of *Deprea*: New insights into the evolutionary history of physaloid groups. *Molecular Phylogenetics and Evolution* 119: 71–80.

Deanna, R., A. Orejuela, and G. E. Barboza. 2018a. An updated phylogeny of *Deprea* (Solanaceae) with a new species from Colombia: Interspecific relationships, conservation assessment and a key for Colombian species. *Systematics and Biodiversity* 16: 680–691.

Deanna, R., S. D. Smith, T. Särkinen, and F. E. Chiarini. 2018b. Patterns of chromosomal evolution in the florally diverse Andean clade Iochrominae (Solanaceae). *Perspectives in Plant Ecology, Evolution and Systematics* 35: 31–43.

De-Silva, D. L., L. L. Mota, N. Chazot, R. Mallarino, K. L. Silva-Brandão, L. M. G. Piñerez, A. V. L. Freitas, et al. 2017. North Andean origin and diversification of the largest Ithomiine butterfly genus. *Scientific Reports* 7: 45966.

Doyle, J. J., and J. L. Doyle. 1987. A rapid procedure for DNA purification from small quantities of fresh leaf tissue. *Phytochemical Bulletin* 19: 11–15.

Drummond, A. J., S. Y. W. Ho, M. J. Phillips, and A. Rambaut. 2006b. Relaxed phylogenetics and dating with confidence. *PLoS Biology* 4: e88.

Drummond, A. J., M. Kearse, J. Heled, R. Moir, T. Thierer, B. Ashton, A. Wilson, and S. Stones-Havas. 2006a. Geneious v4.6.1. Biomatters, Auckland, New Zealand.

Edgar, R. C. 2004. MUSCLE: Multiple sequence alignment with high accuracy and high throughput. *Nucleic Acids Research* 32: 1792–1797.

Eriksson, O., E. M. Friis, and P. Löfgren. 2000. Seed size, fruit size, and dispersal systems in angiosperms from the Early Cretaceous to the Late Tertiary. *The American Naturalist* 156: 47–58.

Fernandez-Hilario, R., and S. D. Smith. 2017. A new species of *Saracha* (Solanaceae) from the Central Andes of Peru. *PhytoKeys* 85: 31–43.

FitzJohn, R. G. 2012. Diversitree: Comparative phylogenetic analyses of diversification in R. *Methods in Ecology and Evolution* 3: 1084–1092.

Francis, J. K. 2000. *Hernandia sonora* L. Mago, toporite Hernandiaceae Familia de las hernandias. *General Technical Report IITF* 15: 260.

Fritz, S. A., and A. Purvis. 2010. Selectivity in mammalian extinction risk and threat types: A new measure of phylogenetic signal strength in binary traits. *Conservation Biology* 24: 1042–1051.

Gautier-Hion, A., J.-M. Duplantier, R. Quris, F. Feer, C. Sourd, J.-P. Decoux, G. Dubost, et al. 1985. Fruit characters as a basis of fruit choice and seed dispersal in a tropical forest vertebrate community. *Oecologia* 65: 324–337.

Gernhard, T. 2008. The conditioned reconstructed process. *Journal of Theoretical Biology* 253: 769–778.

Givnish, T. J., J. C. Pires, S. W. Graham, M. A. McPherson, L. M. Prince, T. B. Patterson, H. S. Rai, et al. 2005. Repeated evolution of net venation and fleshy fruits among monocots in shaded habitats confirms a priori predictions: Evidence from an *ndhF* phylogeny. *Proceedings of the Royal Society B* 272: 1481–1490.

Gottschling, M., and J. S. Miller. 2006. Clarification of the taxonomic position of *Auxemma*, *Patagonula*, and *Saccellium* (Cordiaceae, Boraginales). *Systematic Botany* 31: 361–367.

Hall, J. C., T. E. Tisdale, K. Donohue, A. Wheeler, M. A. Al-Yahya, and E. M. Kramer. 2011. Convergent evolution of a complex fruit structure in the tribe Brassiceae (Brassicaceae). *American Journal of Botany* 98: 1989–2003.

He, C., and H. Saedler. 2005. Heterotopic expression of *MPF2* is the key to the evolution of the Chinese lantern of *Physalis*, a morphological novelty in Solanaceae. *Proceedings of the National Academy of Sciences USA* 102: 5779–5784.

He, C., and H. Saedler. 2007. Hormonal control of the inflated calyx syndrome, a morphological novelty, in *Physalis*. *The Plant Journal* 49: 935–946.

He, C., T. Münster, and H. Saedler. 2004. On the origin of floral morphological novelties. *FEBS Letters* 567: 147–151.

Hepper, N. F. 1991. Old World *Withania* (Solanaceae): A taxonomic review and key to the species. *In* J. G. Hawkes, R. N. Lester, M. Nee, and N. Estrada [eds.], Solanaceae III: Taxonomy, chemistry, evolution, 211–227. Royal Botanic Gardens & Linnean Society of London, London, UK.

Hu, J.-Y., and H. Saedler. 2007. Evolution of the inflated calyx syndrome in Solanaceae. *Molecular Biology and Evolution* 24: 2443–2453.

Hua, X., and L. Bromham. 2016. Phylometrics: An R package for detecting macroevolutionary patterns, using phylogenetic metrics and backward tree simulation. *Methods in Ecology and Evolution* 7: 806–810.

Huelsenbeck, J. P., R. Nielsen, and J. P. Bollback. 2003. Stochastic mapping of morphological characters. *Systematic Biology* 52: 131–158.

Hunziker, A. 1969. Estudios sobre Solanaceae V. Contribución al conocimiento de *Capsicum* y géneros afines (*Witheringia*, *Acnistus*, *Athenaea*, etc.). Primera parte. *Kurtziana* 5: 101–179.

Hunziker, A. T. 2001. Genera Solanacearum. A.R.G. Gantner, Ruggell, Germany.

Iqbal, M., and A. K. Datta. 2007. Cytogenetic studies in *Withania somnifera* (l.) Dun. (Solanaceae). *Cytologia* 72: 43–47.

Khan, M. R., J.-Y. Hu, S. Riss, C. He, and H. Saedler. 2009. *MPF2*-like-A MADS-box genes control the inflated calyx syndrome in *Withania* (Solanaceae): Roles of Darwinian selection. *Molecular Biology and Evolution* 26: 2463–2473.

Khan, M. R., J. Hu, and G. M. Ali. 2012a. Reciprocal loss of CArG-boxes and auxin response elements drives expression divergence of *MPF2*-Like MADS-box genes controlling calyx inflation. *PLoS One* 7: e42781.

Khan, M. R., J. Hu, and C. He. 2012b. Plant hormones including ethylene are recruited in calyx inflation in solanaceous plants. *Journal of Plant Physiology* 169: 940–948.

Khan, M. R., I. U. Khan, and G. M. Ali. 2013. *MPF2*-like MADS-box genes affecting expression of SOC1 and MAF1 are recruited to control flowering time. *Molecular Biotechnology* 54: 25–36.

Knapp, S. 2002. Tobacco to tomatoes: A phylogenetic perspective on fruit diversity in the Solanaceae. *Journal of Experimental Botany* 53: 2001–2022.

Lagomarsino, L. P., F. L. Condamine, A. Antonelli, A. Mulch, and C. C. Davis. 2016. The abiotic and biotic drivers of rapid diversification in Andean bellflowers (Campanulaceae). *New Phytologist* 210: 1430–1442.

Larson-Johnson, K. 2016. Phylogenetic investigation of the complex evolutionary history of dispersal mode and diversification rates across living and fossil Fagales. *New Phytologist* 209: 418–435.

Leiva González, S., and P. Lezama. 2005. *Iochroma albianthum* e *Iochroma ayabacense* (Solanaceae: Solaneae) dos nuevas especies del Departamento de Piura, Perú. *Arnaldoa* 12: 72–80.

Leiva Gonzalez, S., P. Lezama Asencio, and V. Quipuscoa Silvestre. 2003. *Iochroma salpoanum* y *I. squamosum* (Solanaceae: Solaneae) dos nuevas especies andinas del norte del Perú. *Arnaldoa* 10: 95–104.

Leiva González, S., R. Deanna, and J. J. Gavilán. 2013. Tres nuevas especies de *Iochroma* Bentham (Solanaceae) del Norte del Perú. *Arnaldoa* 20: 25–44.

Lezama Escobedo, K., E. Pereyra Villanueva, S. Limo Cruz, and S. Leiva Gonzalez. 2007. *Iochroma smithianum* (Solanaceae) una nueva especie del Departamento La Libertad, Peru. *Arnaldoa* 14: 23–28.

Li, H.-Q., P. Gui, S.-Z. Xiong, and J. E. Averett. 2013. The generic position of two species of tribe Physaleae (Solanaceae) inferred from three DNA sequences: A case study on *Physaliastrum* and *Archiphysalis*. *Biochemical Systematics and Ecology* 50: 82–89.

Lomáscolo, S. B., D. J. Levey, R. T. Kimball, B. M. Bolker, and H. T. Alborn. 2010. Dispersers shape fruit diversity in *Ficus* (Moraceae). *Proceedings of the National Academy of Sciences USA* 107: 14668–14672.

Marcussen, T., and A. S. Meseguer. 2017. Species-level phylogeny, fruit evolution and diversification history of *Geranium* (Geraniaceae). *Molecular Phylogenetics and Evolution* 110: 134–149.

Mason-Gamer, R. J., and E. A. Kellogg. 1996. Testing for phylogenetic conflict among molecular data sets in the tribe Triticeae (Gramineae). *Systematic Biology* 45: 524–545.

Miller, M. A., W. Pfeiffer, and T. Schwartz. 2010. Creating the CIPRES Science Gateway for inference of large phylogenetic trees. *In* Gateway Computing Environments Workshop (GCE), 1–8, IEEE.

Ng, J., and S. D. Smith. 2014. How traits shape trees: New approaches for detecting character state-dependent lineage diversification. *Journal of Evolutionary Biology* 27: 2035–2045.

Olmstead, R. G., L. Bohs, H. Abdel Migid, E. Santiago-Valentín, V. F. Garcia, and S. M. Collier. 2008. A molecular phylogeny of the Solanaceae. *Taxon* 57: 1159–1181.

Ortiz-Ramírez, C. I., S. Plata-Arboleda, and N. Pabón-Mora. 2018. Evolution of genes associated with gynoecium patterning and fruit development in Solanaceae. *Annals of Botany* 121: 1211–1230.

Pabón-Mora, N., G. K.-S. Wong, and B. A. Ambrose. 2014. Evolution of fruit development genes in flowering plants. *Frontiers in Plant Science* 5: 300.

Padmaja, H., S. Sruthi, and M. Vangalapati. 2014. Review on *Hibiscus sabdariffa*-A valuable herb. *International Journal of Pharmacy & Life Sciences* 5: 3747–3752.

Paradis, E., J. Claude, and K. Strimmer. 2004. APE: Analyses of Phylogenetics and Evolution in R language. *Bioinformatics* 20: 289–290.

Paton, A. 1990. A global taxonomic investigation of *Scutellaria* (Labiatae). *Kew Bulletin* 45: 399–450.

Poczai, P., and J. Hyvönen. 2011. Identification and characterization of plastid *trnF* (GAA) pseudogenes in four species of *Solanum* (Solanaceae). *Biotechnology Letters* 33: 2317.

Posada, D., and K. A. Crandall. 1998. Modeltest: Testing the model of DNA substitution. *Bioinformatics* 14: 817–818.

Rambaut, A. 2016. FigTree, version 1.4.3. Computer program and documentation distributed by the author. http://tree.bio.ed.ac.uk/software/figtree/.

Rambaut, A., A. J. Drummond, D. Xie, G. Baele, and M. A. Suchard. 2018. Posterior summarisation in Bayesian phylogenetics using Tracer 1.7. *Systematic Biology* 67: 901–904.

Revell, L. J. 2012. phytools: An R package for phylogenetic comparative biology (and other things). *Methods in Ecology and Evolution* 3: 217–223.

Riss, S. 2009. Isolation and analysis of *MPF2*-like MADS-box genes from Physaleae and characterization of their cis-regulatory regions. Ph.D. dissertation, Universität zu Köln, Köln, Germany.

Särkinen, T., L. Bohs, R. G. Olmstead, and S. Knapp. 2013. A phylogenetic framework for evolutionary study of the nightshades (Solanaceae): A dated 1000-tip tree. *BMC Evolutionary Biology* 13: 214–229.

Särkinen, T., S. Kottner, W. Stuppy, F. Ahmed, and S. Knapp. 2018. A new commelinid monocot seed fossil from the early Eocene previously identified as Solanaceae. *American Journal of Botany* 105: 95–107.

Sawyer, N. W. 2001. New species and combinations in *Larnax* (Solanaceae). *Novon* 11: 460–471.

Schliep, K. P. 2011. phangorn: Phylogenetic analysis in R. *Bioinformatics* 27: 592–593.

Shaw, J. 2018a. *Iochroma* reshuffle. *The Plantsman* 17: 124–125.

Shaw, J. 2018b. Response from Julian Shaw, Senior Registrar, RHS Botany Department. *The Plantsman* 17: 200.

Smith, S. D., and D. A. Baum. 2006. Phylogenetics of the florally diverse Andean clade Iochromidae (Solanaceae). *American Journal of Botany* 93: 1140–1153.

Smith, S. D., C. Ane, and D. A. Baum. 2008. The role of pollinator shifts in the floral diversification of *Iochroma* (Solanaceae). *Evolution* 62: 793–806.

Stamatakis, A. 2014. RAxML version 8: A tool for phylogenetic analysis and post-analysis of large phylogenies. *Bioinformatics* 30: 1312–1313.

Stenz, N. W. M., B. Larget, D. A. Baum, and C. Ané. 2015. Exploring tree-like and non-tree-like patterns using genome sequences: An example using the inbreeding plant species *Arabidopsis thaliana* (L.) Heynh. *Systematic Biology* 64: 809–823.

Tamura, K., G. Stecher, D. Peterson, A. Filipski, and S. Kumar. 2013. MEGA6: Molecular evolutionary genetics analysis version 6.0. *Molecular Biology and Evolution* 30: 2725–2729.

Tewksbury, J. J., and G. P. Nabhan. 2001. Seed dispersal: Directed deterrence by capsaicin in chillies. *Nature* 412: 403.

Tiffney, B. H. 1984. Seed size, dispersal syndromes, and the rise of the angiosperms: Evidence and hypothesis. *Annals of the Missouri Botanical Garden* 71: 551–576.

Traveset, A. 1998. Effect of seed passage through vertebrate frugivores' guts on germination: A review. *Perspectives in Plant Ecology, Evolution and Systematics* 1: 151–190.

Turner, B. L. 2015. Taxonomy of *Chamaesaracha* (Solanaceae). *Phytologia* 97: 226–245.

Vaidya, G., D. J. Lohman, and R. Meier. 2011. SequenceMatrix: Concatenation software for the fast assembly of multi-gene datasets with character set and codon information. *Cladistics* 27: 171–180.

Vander Wall, S. B. 2001. The evolutionary ecology of nut dispersal. *The Botanical Review* 67: 74–117.

Wang, L., J. Li, J. Zhao, and C. He. 2015. Evolutionary developmental genetics of fruit morphological variation within the Solanaceae. *Frontiers in Plant Science* 6: 248.

Whitson, M., and P. S. Manos. 2005. Untangling *Physalis* (Solanaceae) from the physaloids: A two-gene phylogeny of the Physalinae. *Systematic Botany* 30: 216–230.

Wilf, P., M. R. Carvalho, M. A. Gandolfo, and N. R. Cúneo. 2017. Eocene lantern fruits from Gondwanan Patagonia and the early origins of Solanaceae. *Science* 355: 71–75.

Zamberlan, P. M., I. Rodrigues, G. Mäder, L. Castro, J. R. Stehmann, S. L. Bonatto, and L. B. Freitas. 2015. Re-evaluation of the generic status of *Athenaea* and *Aureliana* (Withaniinae, Solanaceae) based on molecular phylogeny and morphology of the calyx. *Botanical Journal of the Linnean Society* 177: 322–334.

Zamora-Tavares, M. del P., M. Martínez, S. Magallón, L. Guzmán-Dávalos, and O. Vargas-Ponce. 2016. *Physalis* and physaloids: A recent and complex evolutionary history. *Molecular Phylogenetics and Evolution* 100: 41–50.

Zhang, J., M. R. Khan, Y. Tian, Z. Li, S. Riss, and C. He. 2012. Divergences of *MPF2*-like MADS-domain proteins have an association with the evolution of the inflated calyx syndrome within Solanaceae. *Planta* 236: 1247–1260.